

# From 3D Point Clouds to Climbing Stairs: A Comparison of Plane Segmentation Approaches for Humanoids

Stefan Oßwald

Jens-Steffen Gutmann

Armin Hornung

Maren Bennewitz

**Abstract**—In this paper, we consider the problem of building 3D models of complex staircases based on laser range data acquired with a humanoid. These models have to be sufficiently accurate to enable the robot to reliably climb up the staircase. We evaluate two state-of-the-art approaches to plane segmentation for humanoid navigation given 3D range data about the environment. The first approach initially extracts line segments from neighboring 2D scan lines, which are successively combined if they lie on the same plane. The second approach estimates the main directions in the environment by randomly sampling points and applying a clustering technique afterwards to find planes orthogonal to the main directions. We propose extensions for this basic approach to increase the robustness in complex environments which may contain a large number of different planes and clutter. In practical experiments, we thoroughly evaluate all methods using data acquired with a laser-equipped Nao robot in a multi-level environment. As the experimental results show, the reconstructed 3D models can be used to autonomously climb up complex staircases.

## I. INTRODUCTION

Humanoid robots envisioned to autonomously act in environments designed for humans must be able to climb stairs in order to reach upper levels in multi-story buildings. As a prerequisite, the robots have to be able to acquire accurate models of staircases. In a previous work [1], we presented an approach to autonomous stair climbing with humanoids given a known 3D model of the whole staircase. In this paper, our goal is to build accurate models of complex staircases based on the robot's sensor data. We rely on 3D laser range data and aim at extracting planes corresponding to stairs from the 3D point cloud to reconstruct a model of the staircase.

We adapt, evaluate, and compare two approaches to plane extraction on our humanoid platform. These approaches have been successfully applied to humanoid navigation on non-flat ground in the past. The first approach was presented by Gutmann *et al.* [2]. It is based on scan-line grouping and first extracts line segments from neighboring scan lines in a range image. The line segments are successively combined to plane segments if they lie on the same plane. This algorithm is highly efficient since it relies on the initially extracted line segments rather than on repeated processing of the 3D points.

The second approach was developed by Kida *et al.* [3] and relies on two-point random sampling. This method directly operates on the 3D point cloud. The key idea here is to

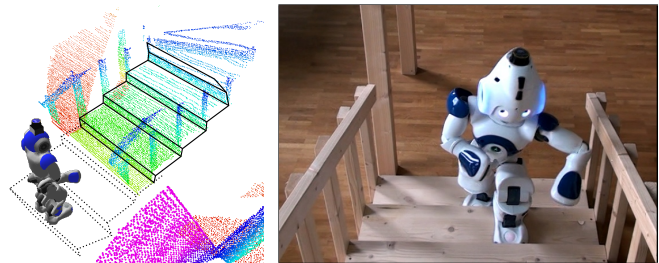


Fig. 1. *Left:* Model of the staircase reconstructed from a 3D point cloud acquired with a laser-equipped Nao humanoid. *Right:* The robot is able to climb the staircase based on the learned model of the environment.

estimate main directions in the environment by randomly sampling points and determining their difference vectors. Afterwards, the authors apply a clustering technique to find plane segments that are orthogonal to the main directions. We propose four modifications of this two-point random sampling method to increase the robustness in complex environments containing multiple planes and clutter.

Other approaches for plane segmentation are based on Expectation Maximization (EM) [4], [5] or RANSAC [6], but are not covered in detail in this work. EM for plane segmentation is time-consuming to compute for large point clouds and thus not practical in our scenario. RANSAC, in our experience, tends to over-simplify complex planar structures. For example, multiple small steps are often merged into one sloped plane.

We evaluated scan-line grouping and the improved version of two-point random sampling in extensive experiments using 3D laser data acquired by our Nao humanoid robot. As the experiments show, both methods show comparable good results and lead to 3D models that can be used for autonomous climbing of complex staircases with humanoids (see Fig. 1).

The paper is organized as follows. In the next section, we discuss related work on climbing stairs and plane segmentation from distance data. In Sec. III, we describe the data acquisition process with the Nao humanoid and in Sec. IV and V we present the two plane extraction techniques as well as our proposed improvements. Finally, we show and discuss experimental results in Sec. VI.

## II. RELATED WORK

We first discuss techniques for humanoid stair climbing. Several approaches do not use a 3D model at all. For example, Nishiwaki *et al.* [7] constructed toe joints for the humanoid H7. H7 was able to climb single steps after manually positioning the robot in front of them. Honda's

Stefan Oßwald, Armin Hornung, and Maren Bennewitz are with the Humanoid Robots Lab, University of Freiburg, Germany. Jens-Steffen Gutmann is with Evolution Robotics Inc. in Pasadena, USA. Part of this research originates from his work at Sony Corp. in Tokyo, Japan.

This work has partly been supported by the German Research Foundation (DFG) under contract number SFB/TR-8.

ASIMO [8] executes a fixed sequence of footsteps that is locally adapted using data from force sensors.

Michel *et al.* [9] proposed to visually track single objects that are in the camera's field of view. This approach is based on a given 3D model and a matching between detected and model edges. After a manual pose initialization, the robot can determine its pose relative to the tracked object, e.g., the staircase. Their HRP-2 climbed up staircases with three steps. Cupec *et al.* [10] developed a vision-based approach to track obstacles. Obstacle detection relies on the assumption that obstacles and floor are clearly distinguishable in the images to simplify edge detection. The authors presented experiments in which the robot Johnnie climbed two steps which were reconstructed in 3D.

Okada *et al.* [11] proposed a technique to reconstruct single steps from 3D stereo data. The authors used a randomized 3D Hough transform to extract planes. Their humanoid autonomously climbed a single step. Gutmann *et al.* [12] use the efficient scan-line grouping algorithm [2] discussed in this paper to extract models of steps given stereo data. Using such models, the humanoid QRIO was able to climb up and down staircases consisting of four steps. Chestnutt *et al.* [13] applied the two-point random sampling method [3] also evaluated in this paper to identify planes corresponding to steps or flat obstacles based on 3D laser point cloud data. To speed-up the process, they restricted the detection to planes  $\pm 30^\circ$  from horizontal and used lookup templates specific to the environment when sampling. Their humanoid robot equipped with a pivoting laser scanner was able to climb up and down two successive steps of a small staircase.

Furthermore, there are general approaches for segmentation of 3D range data. Hähnel *et al.* [14] apply a region-growing technique to identify planes in 3D point clouds. The main focus was here to generate compact models of buildings. EM-based procedures to extract planes from 3D range data as proposed, for example, by Triebel *et al.* [4] and Thrun *et al.* [5] are rather time-consuming since the data points need to be processed multiple times during the estimation of the model components and also for the estimation of the number of components.

Rusu *et al.* [6] proposed to divide the point cloud into different cells and apply RANSAC to find polygons locally which are merged afterwards. The resulting polygonal models were used for navigation with the ground-based RHex robot. RANSAC, however, tends to over-simplify complex planar structures in our experience. Multiple small steps are often merged into one sloped plane which is inappropriate for safely climbing stairs with a humanoid. Klasing *et al.* [15] developed a technique to surface segmentation given a continuous stream of 3D range data. The authors compute normal vectors of points given a local neighborhood and cluster the points afterwards based on their distance. The results are quite impressive, however, they highly depend on the choice of different parameters as stated by the authors.

The recent work of Ben-Tzvi *et al.* [16] follows a different approach. The authors first generate a depth image from the 3D point cloud and reconstruct contours of objects. Afterwards, they segment planes based on the contours. The



Fig. 2. *Left:* The two-level environment in which the robot is navigating. *Right:* The Nao humanoid is acquiring a 3D point cloud of the environment by tilting its head with the 2D laser range finder on top.

technique works well for scenes with a low number of planes, however, it is unclear how it scales to more complex scenes.

### III. DATA ACQUISITION

For our experiments, we use a Nao humanoid equipped with two monocular cameras and a Hokuyo URG-04LX laser range finder. The sensor is mounted on the top of the humanoid's head and provides 2D range data in a field of view of  $240^\circ$  at  $0.33^\circ$  resolution with an update rate of 10 Hz. With this modified head, Nao is 64 cm tall.

Our robot is navigating in a two-level environment connected by a spiral staircase with ten steps (see Fig. 2, left). By tilting its head and combining the 2D scans, the robot obtains 3D point cloud data of the environment (see Fig. 2, right). Note that there is a minimum distance of 50 cm between the laser plane and the robot's feet when scanning due to the placement of the scanner on the head. Fig. 3 illustrates an example 3D scan projected on a manually constructed CAD model of the staircase. In this case, the robot was standing close to the first step. As can be seen, only the third step is completely represented in the data. Whereas the first step and parts of the second one are outside the robot's field of view, the higher steps suffer from partial occlusions. Therefore, in practice the robot has to acquire a new scan every two steps to be able to build an accurate model of the staircase. Fig. 4 visualizes the data from the side. Shown is an orthographic projection of the 3D scan of a small staircase with three steps. As can be seen, the data is highly noisy with errors up to 5 cm which makes plane fitting a challenging task. The noise originates from the inaccuracy of the laser scanner itself [17] as well as from the estimation of the sensor's pose from forward kinematics based on the joint angles while tilting the head.

### IV. SCAN-LINE GROUPING

A fast and efficient method for extracting planes from a range image is to first fit straight line segments to each image row and then perform region growing using the lines as primitives to form planar regions. The approach was originally presented by Jiang and Bunke [18] and performed best in a comparison with other earlier range segmentation techniques [19]. Since then the algorithm has been extended and improved in order to deal with range data containing varying levels of noise, such as range images obtained from stereo vision [2]. The method has successfully been applied on Sony's QRIO robot, allowing the humanoid to recognize

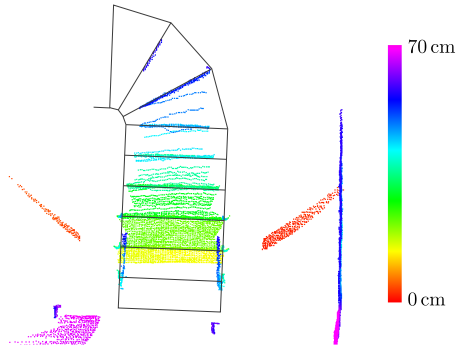


Fig. 3. Projection of the acquired 3D point cloud on a manually constructed 3D model of the staircase for visualization of the data. During data acquisition, the robot was standing directly in front of the first step.

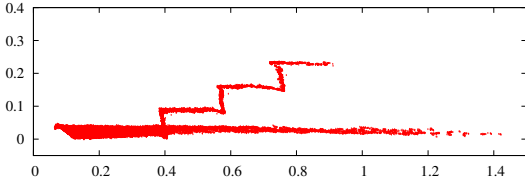


Fig. 4. Side view of 3D point cloud corresponding to a staircase with three steps, each 7 cm high. As can be seen, the data suffers from noise which poses challenges on the plane fitting.

floor, stairs, obstacles, and tables, and to plan and navigate its path on an obstacle course [20].

In this work we investigate how well the method is suited to the data taken by Nao's laser range finder. For this purpose we slightly extend the method to deal with the specific data acquisition procedure on the Nao humanoid. Fig. 5 shows a flow chart of the algorithm.

In the first step, the range scans are assembled into a range image where each pixel holds a 3D point in a coordinate system aligned with the image plane. The advantage of such an image representation is that the contours of regions can be found by looking at the 3D points of neighboring pixels. As the laser readings are collected by tilting the head of the robot, a range image can be assembled by sorting the individual range scans by the pitch angle of the neck joint. In order to obtain more homogeneous data, scans with a similar pitch angle (difference less than  $0.18^\circ$ )<sup>1</sup> are discarded.

Note that the creation of a range image becomes more involved as the trajectory of the range finder becomes more complex, e.g. when also yaw and roll of the head are changing. In fact, if the robot were to walk while collecting the range scans, a range image representing the full 3D data might not exist due to the possible occlusion of objects.

In the second step, line segments are fit to each range scan (image row). This is achieved by partitioning the 3D points into groups where a new group is started whenever the distance between neighboring points exceeds a threshold (5 cm). For each group, a straight line is computed by least squares optimization. Using a run distribution test, the accuracy of the line is evaluated: if more than a number (15) of consecutive points all fall on one side of the line, the group

<sup>1</sup>Numbers in parentheses indicate the values of parameters used in our experiments in Sec. VI.

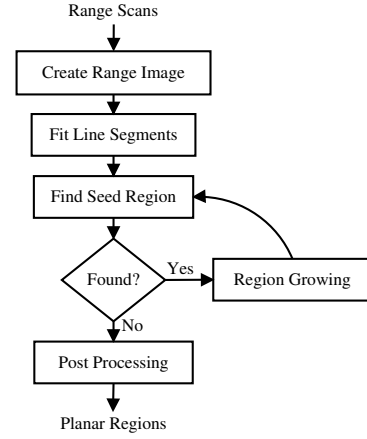


Fig. 5. Flow-chart of scan-line grouping used in this research. Except for the initial conversion into a range image, the system is identical to the method on Sony's QRIO robot [2].

is split at the point most distant to the chord connecting start and end point of the group. The algorithm then processes each sub-group recursively. Lines with less than a number of points (5) or shorter than a threshold (5 cm) are discarded.

The extraction of a plane starts by finding three line segments in neighboring image rows that overlap in their start and end columns. The three lines must pass a statistical test before considering them as a seed for a plane: the standard deviation of the plane fit to all points of the three lines (using least squares) must not be larger than a factor (2) of the standard deviation of each line. Once a seed region has been determined, a region growing procedure is performed that adds lines in neighboring rows and columns to the plane as long as the standard deviation of the line points with respect to the plane is less than a factor (2.5) of the standard deviation of the line itself.

When no more seed regions can be found, the scan-line grouping algorithm terminates. In a post processing step, the found planes are refined. This includes checking whether line segments or single data points better fit to a neighboring plane, the merging of co-linear planes, and plane optimization by discarding border pixels. For a complete description, we refer to the original publication [2].

An interesting property of scan-line grouping is that most input points are accessed only when fitting line segments. This makes the algorithm extremely fast as we will see in our experimental results.

## V. TWO-POINT RANDOM SAMPLING

Two-point random sampling as introduced by Kida *et al.* [3] relies on the assumption that, in man-made environments, most surfaces are aligned with respect to a small set of main directions. To exploit this information, the two-point random sampling algorithm first determines the main directions of the point cloud by sampling. Then, the algorithm cuts the data into slices perpendicular to each main direction and searches for plane segments within each slice. Note that we can not simply assume planes perpendicular to the  $z$  normal because the scan may be tilted due to small errors in the robot's pose, and because the front faces of the



steps are also important for the extraction.

#### A. Basic Algorithm

Given a set of points  $\mathbf{p}_1, \dots, \mathbf{p}_N$ , the algorithm extracts plane segments as follows.

- 1) Sample a set  $V$  of normalized difference vectors ( $|V| = 10000$ ):

$$V \leftarrow \left\{ \frac{\mathbf{p}_i - \mathbf{p}_j}{\|\mathbf{p}_i - \mathbf{p}_j\|} \mid 1 \leq i, j \leq N, i \neq j \right\} \quad (1)$$

The elements of  $V$  can be interpreted as points on the unit sphere. Points  $\mathbf{p}_i, \mathbf{p}_j$  originating from different surfaces in the environment generate randomly distributed points on the unit sphere. If  $\mathbf{p}_i$  and  $\mathbf{p}_j$  both originate from a common flat surface in the environment, then the corresponding point in  $V$  is located on the unit circle with the same normal vector as the surface. Hence, all points drawn from surfaces with similar normal vectors produce rings with a high point density on the unit sphere. By considering the point density, planar surfaces can be distinguished from the noise occurring in the data.

- 2) Find a ring-shaped cluster  $R = \{\mathbf{v}_1, \dots, \mathbf{v}_M\} \subseteq V$ .
- 3) Determine the normal vector of  $R$  by optimizing:

$$\mathbf{n} \leftarrow \arg \max_{\mathbf{n}} \sum_{k=1}^M \begin{cases} 1 & \text{if } \mathbf{n}^T \mathbf{v}_k \approx 0 \\ 0 & \text{otherwise} \end{cases} \quad (2)$$

- 4) Cut the point cloud into thin slices perpendicular to  $\mathbf{n}$ .
- 5) For each slice containing a sufficient number of points (20): Cluster the points within the slice to plane segments.

Repeat Steps 2) to 5) to find further planes.

#### B. Improved Version

While the basic algorithm is sufficient for scenes containing a moderate number of planes, the robustness has to be improved for more complex scenes containing many planes or clutter. In this paper, we propose four improvements to increase the robustness.

- 1) During the sampling step, the original algorithm draws pairs of points randomly from the whole point cloud. In more complex environments, the probability that both points originate from the same surface is low, so that the resulting rings on the unit sphere are not dense enough to be easily distinguishable from the noise in the data. Additionally, the directions of the difference vectors are biased if the dimensions of the environment are not approximately equal. Drawing the second point  $\mathbf{p}_j$  from the nearest neighbors of the first point  $\mathbf{p}_i$  with  $d_1 \leq \text{dist}(\mathbf{p}_i, \mathbf{p}_j) \leq d_2$  ( $d_1 = 2$  cm,  $d_2 = 7$  cm) increases the probability that both points originate from the same surface and reduces the bias. The lower boundary reduces the susceptibility to noise. Fig. 6 shows the elements of  $V$  as points on the unit sphere. The point cloud was acquired with a 3D laser scan in our two-level environment depicted in Fig. 2. As can be seen, when using uniform sampling, the main directions

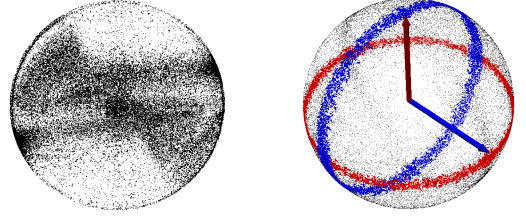


Fig. 6. The normalized difference vectors  $V$  from the point cloud in Fig. 3 as points on the unit sphere (black dots). *Left:* With uniform sampling, there are no distinct main directions. *Right:* Using improved sampling considering neighboring information, the distinct rings corresponding to the main directions can be clearly identified (indicated by their normal vectors as red and blue arrows).

cannot be reliably estimated. In contrast, our sampling strategy that considers neighborhood information leads to clearly distinguishable rings corresponding to the main direction.

- 2) We combine V-A Step 2) and 3) by applying RANSAC to estimate the main directions. Here, we repeatedly sample two points in  $V$  and determine their normal vector to find the main directions.
- 3) In complex environments, the slices that are considered in V-A Step 5) may contain columns and handrails or intersect planes that are perpendicular to the slice. The algorithm might mistake these objects for small plane segments, as they contain a similar number of points. Therefore, we analyze the eigenvalues  $\lambda_1 \leq \lambda_2 \leq \lambda_3$  of the segmented points' covariance matrix to reject thin and long plane segments with  $\lambda_3 \gg \lambda_2$ .
- 4) In a final step, we merge neighboring planes that probably originated from the same surface. Due to measurement noise, the points of a single surface may fall into two adjacent slices. As only points within one slice are considered for finding plane segments, these points generate two distinct, parallel plane segments. Hence, we identify and merge planes with similar parameters after the extraction. In particular, planes are merged if their distance is at most 3 cm and their normals have an angular difference of at most  $11^\circ$ .

## VI. EXPERIMENTS

We now discuss experimental results obtained with the two methods presented above given 3D laser data acquired with our humanoid robot as described in Sec. III. As discussed before, the input data contains both random noise and systematic errors caused by the measurement process. This noise equally affects the performance of all algorithms.

For our experimental comparison, we use datasets acquired while the robot was standing at a distance of 70 cm in front of the staircase, and while standing on the first, third, fifth, and seventh step. The datasets consist of approximately 132 000 points each.

#### A. Qualitative Segmentation Results

In our experiments, we found that scan-line grouping as well as the improved version of the two-point algorithm reliably extract most plane segments of the staircase within the robot's field of view (see Figs. 7-10). Since scan-line

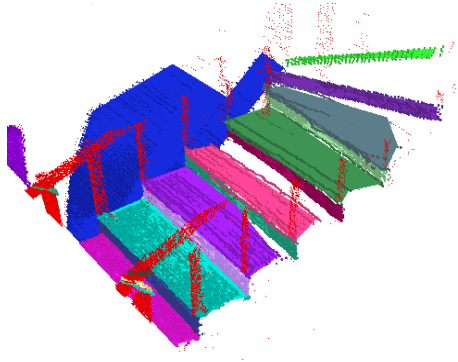


Fig. 7. Result of scan-line grouping on the point cloud of Fig. 3. Each segmented plane is indicated by a different color. The large blue area corresponds to the floor. Points not belonging to a plane are shown in red. Note how the results degrade as data becomes more sparse at higher steps.

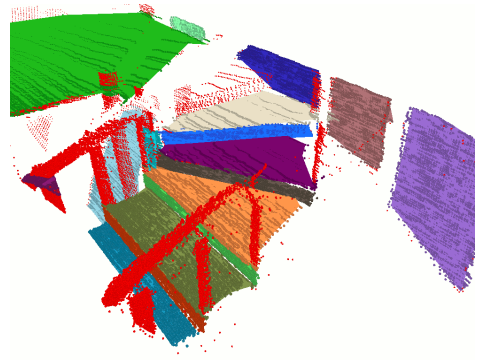


Fig. 8. Segmentation using scan-line grouping on another dataset of the upper part of our spiral staircase. Several steps are extracted successfully including their vertical faces. The large green area corresponds to the upper level whereas segments on the right refer to a distant wall.

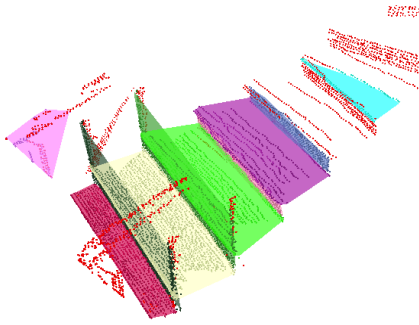


Fig. 9. Result of our improved two-point random sampling method on the point cloud of Fig. 3. The lower stairs are identified reliably. Parts of the hand rails are initially merged to the front faces, but will be removed later when reconstructing the staircase model.

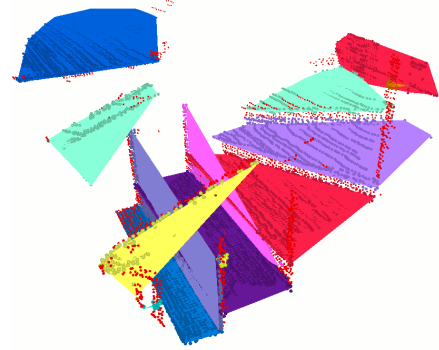


Fig. 10. Segmentation of our improved two-point algorithm on the dataset of the upper staircase. The same steps as in scan-line grouping are segmented reliably. Even though some vertical faces are missing, the extraction result can be used for reconstructing the staircase model.

grouping can find planes with arbitrary orientations, the method in general extracts more plane segments than the two-point algorithm. In most cases, the method also precisely finds the edges of planes due to the refinements carried out in the post-processing step.

On the other hand, the two-point algorithm is also able to detect smaller plane segments as long as they are aligned to one of the main directions. Only small plane segments not parallel to other planes generate sparse rings on the unit sphere making such planes hard to distinguish from random noise. Accordingly, the two-point method is less likely to extract small planes with less frequent orientations such as the vertical faces of the rotating part of our spiral staircase. However, these steps can still be reconstructed from the more reliable detection of the horizontal faces as shown in Fig. 10. Note that, for a clearer visualization, Figs. 7-10 show the convex hulls of the points in the planes.

### B. Quantitative Reconstruction Results

We reconstruct stairs in a straightforward manner as briefly described in the following. First, we intersect horizontal and vertical planes and obtain a set of straight horizontal lines. Next, we determine the boundaries of each line segment by projecting the convex hull of points belonging to a plane onto the lines. Finally, the endpoints of parallel lines are connected to form a stair model.

For the quantitative evaluation, we measured the runtime and compared the reconstructed dimensions of the steps and the angles between adjacent faces to the ground truth of the staircase. Table I shows a summary of the results in terms of average error and standard deviation. The two-point random sampling algorithm aligns all planes with respect to a small number of common main directions, thus the angular deviation between parallel planes tends to be lower than in models generated by scan-line grouping. Both methods lead to stair models that are accurate enough to be climbed autonomously. Regarding computational complexity, the scan-line grouping algorithm is significantly more efficient as it mainly operates on line segments extracted from the range image, whereas sampling-based methods operate on the whole point cloud and need a large number of iterations to find all plane segments with sufficiently high probability.

However, it is worth mentioning that two-point random sampling can also be used to extract plane segments from accumulated point clouds obtained from multiple viewpoints whereas scan-line grouping only operates on one range image from one viewpoint at a time.

### C. Stair Climbing

In order to climb complex staircases, we use the reconstructed 3D model of the whole staircase. To merge models resulting from two independent 3D scans acquired while the

TABLE I  
COMPARISON OF ERROR AND RUNTIME BETWEEN SCAN-LINE  
GROUPING AND TWO-POINT RANDOM SAMPLING

		Scan-Line	Two-Point
		Grouping	Random Sampling
Model Error (avg $\pm$ std)	Step Height (7 cm)	$0.42 \pm 0.31$ cm	$0.68 \pm 0.54$ cm
	Step Width (60 cm)	$3.40 \pm 1.95$ cm	$2.25 \pm 1.97$ cm
	Step Depth (18 cm)	$1.17 \pm 0.67$ cm	$0.90 \pm 0.61$ cm
	Parallel Planes	$2.22 \pm 2.17^\circ$	$1.14 \pm 1.13^\circ$
	90° Angles	$4.97 \pm 2.13^\circ$	$3.12 \pm 1.47^\circ$
Runtime		$0.025 \pm 0.001$ s	$3.102 \pm 1.043$ s

robot is climbing the stairs, we replace steps with newly extracted steps that have the same height level. The result of such a process can be seen in the left image of Fig. 1.

Subsequently, our robot can use the model to autonomously climb up complex staircases. The height of the stairs to step on is thereby given by the model. Since the motions of humanoids are typically executed inaccurately and suffer from drift, the robot needs to integrate new observations in order to accurately position itself and place its feet on the individual steps. This is especially important when climbing the spiral part of the staircase. Otherwise, the robot might bump into the handrail when not being in the center of the steps or slip off the stair edge. For this purpose, our humanoid combines a laser-based localization [21] with observations from its lower camera that covers the area directly in front of its feet. Extracted line segments are matched to the edges of the staircase model to accurately determine the robot's pose on the staircase. Details of this process are described in our previous work [1]. By using the reconstructed model of the staircase and local visual observations in addition, the robot is able to reliably climb the stairs as depicted in Fig. 1. Note that our humanoid cannot use the laser scanner to sense the next step during stair climbing since there is a minimum distance of 50 cm between the laser plane and the feet.

## VII. CONCLUSIONS AND FUTURE WORK

In this paper, we investigated how a humanoid robot with 3D sensing capabilities can perceive staircases in complex environments and reconstruct a 3D model accurately enough in order to climb the staircase safely. We compared and extended two approaches, scan-line grouping and two-point random sampling. Both techniques lead to accurate 3D models despite noisy sensor data, a high number of faces, and clutter in the environment. The learned stair model is slightly more accurate with two-point random sampling, thus we use this approach in practice. As we showed in the experiments, our laser-equipped Nao humanoid is able to reliably sense and climb complex staircases using the methods outlined in this paper. While we mainly focus on data obtained by tilting a 2D laser, all methods are general enough to be applicable to other 3D or depth sensors which are currently becoming more and more available.

## REFERENCES

- [1] S. Obwald, A. Görög, A. Hornung, and M. Bennewitz, "Autonomous climbing of spiral staircases with humanoids," in *Proc. of the IEEE/RSJ Int. Conf. on Intelligent Robots and Systems (IROS)*, 2011.
- [2] J.-S. Gutmann, M. Fukuchi, and M. Fujita, "3D perception and environment map generation for humanoid robot navigation," *The International Journal of Robotics Research (IJRR)*, vol. 27, no. 10, pp. 1117–1134, 2008.
- [3] Y. Kida, S. Kagami, T. Nakata, M. Kouchi, and H. Mizoguchi, "Human finding and body property estimation by using floor segmentation and 3D labelling," in *Proc. of the IEEE Int. Conf. on Systems, Man, and Cybernetics (SMC)*, 2004.
- [4] R. Triebel, W. Burgard, and F. Dellaert, "Using hierarchical EM to extract planes from 3D range scans," in *Proc. of the IEEE Int. Conf. on Robotics & Automation (ICRA)*, 2005.
- [5] S. Thrun, C. Martin, Y. Liu, D. Hähnel, R. Emery-Montemerlo, D. Chakrabarti, and W. Burgard, "A real-time expectation maximization algorithm for acquiring multi-planar maps of indoor environments with mobile robots," *IEEE Trans. on Robotics and Automation*, 2003.
- [6] R. B. Rusu, A. Sundaresan, B. Morisset, K. Hauser, M. Agrawal, J.-C. Latombe, and M. Beetz, "Leaving flatland: Efficient real-time three-dimensional perception and motion planning," *Journal of Field Robotics*, vol. 26, no. 10, pp. 841–862, 2009.
- [7] K. Nishiwaki, S. Kagami, Y. Kuniyoshi, M. Inaba, and H. Inoue, "Toe joints that enhance bipedal and fullbody motion of humanoid robots," in *Proc. of the IEEE Int. Conf. on Robotics & Automation (ICRA)*, 2002.
- [8] K. Hirai, M. Hirose, Y. Haikawa, and T. Takenaka, "The development of Honda humanoid robot," in *Proc. of the IEEE Int. Conf. on Robotics & Automation (ICRA)*, 1998.
- [9] P. Michel, J. Chestnutt, S. Kagami, K. Nishiwaki, J. Kuffner, and T. Kanade, "GPU-accelerated real-time 3D tracking for humanoid locomotion and stair climbing," in *Proc. of the IEEE/RSJ Int. Conf. on Intelligent Robots and Systems (IROS)*, 2007.
- [10] R. Cupec, G. Schmidt, and O. Lorch, "Experiments in vision-guided robot walking in a structured scenario," in *Proc. of the IEEE Int. Symp. on Industrial Electronics*, 2005.
- [11] K. Okada, S. Kagami, M. Inaba, and H. Inoue, "Plane segment finder: Algorithm, implementation and applications," in *Proc. of the IEEE Int. Conf. on Robotics & Automation (ICRA)*, 2001.
- [12] J.-S. Gutmann, M. Fukuchi, and M. Fujita, "Stair climbing for humanoid robots using stereo vision," in *Proc. of the IEEE/RSJ Int. Conf. on Intelligent Robots and Systems (IROS)*, 2004.
- [13] J. Chestnutt, Y. Takaoka, K. Suga, K. Nishiwaki, J. Kuffner, and S. Kagami, "Biped navigation in rough environments using on-board sensing," in *Proc. of the IEEE/RSJ Int. Conf. on Intelligent Robots and Systems (IROS)*, 2009.
- [14] D. Hähnel, W. Burgard, and S. Thrun, "Learning compact 3d models of indoor and outdoor environments with a mobile robot," *Robotics & Autonomous Systems*, vol. 44, no. 1, pp. 15–27, 2003.
- [15] K. Klasing, D. Wollherr, and M. Buss, "Realtime segmentation of range data using continuous nearest neighbors," in *Proc. of the IEEE Int. Conf. on Robotics & Automation (ICRA)*, 2009.
- [16] P. Ben-Tzvi, S. Charifa, and M. Shick, "Extraction of 3D images using pitch-actuated 2D laser range finder for robotic vision," in *Proc. of the IEEE Int. Workshop on Robotic and Sensors Environments (ROSE)*, 2010.
- [17] L. Kneip, F. Tâche, G. Caprari, and R. Siegwart, "Characterization of the compact Hokuyo URG-04LX 2D laser range scanner," in *Proc. of the IEEE Int. Conf. on Robotics & Automation (ICRA)*, 2009.
- [18] X.-Y. Jiang and H. Bunke, "Fast segmentation of range images into planar regions by scan line grouping," *Machine Vision and Applications*, vol. 7, no. 2, pp. 115 – 122, 1994.
- [19] A. Hoover, G. Jean-Baptiste, X. Jiang, P. J. Flynn, H. Bunke, D. B. Goldgof, K. K. Bowyer, D. W. Eggert, A. W. Fitzgibbon, and R. B. Fisher, "An experimental comparison of range image segmentation algorithms," *Transactions on Pattern Analysis and Machine Intelligence*, vol. 18, no. 7, pp. 673 – 689, 1996.
- [20] J.-S. Gutmann, M. Fukuchi, and M. Fujita, "Real-time path planning for humanoid robot navigation," in *Int. Joint Conference on Artificial Intelligence (IJCAI)*, Edinburgh, Scotland, 2005.
- [21] A. Hornung, K. M. Wurm, and M. Bennewitz, "Humanoid robot localization in complex indoor environments," in *Proc. of the IEEE/RSJ Int. Conf. on Intelligent Robots and Systems (IROS)*, 2010.